Synthesis of silica glass fibers and nanoparticles by continuous-wave laser backside irradiation

Namiko Saito[1] · Hirofumi Hidai[1] · Souta Matsusaka[1] · Akira Chiba[1] ·
Noboru Morita[1]

Abstract We have developed a novel method to synthesize fibers and nanoparticles of silica glass using a continuous-wave laser. The synthesis process operates through continuous-wave laser backside irradiation (CW-LBI) of a glass substrate. In CW-LBI, a spindle-shaped emission is generated in the glass bulk along the optical axis; the emission propagates toward the light source as a confined plasma. The emission and its surroundings contain vaporized and molten glass. When the laser irradiation continues for a sufficient duration, the emission forefront reaches the glass surface, at which point vaporized and molten glass are ejected explosively. The ejected glass forms fibers and nanoparticles. Some of the nanoparticles become attached to the fiber surfaces during the explosion. The fiber diameters range from hundreds of nanometers to more than 10 μm. The particles on the fiber surfaces have diameters of tens of nanometers. A spindle-shaped hole remained in the glass substrate after the ejection, which had a depth of ∼3.8 mm. This result indicated that the ejected materials originated from deep inside the glass bulk. High-speed camera observations of the ejection process and scanning electron microscopy of the ejected materials indicated that the fibers formed from the extraction from molten silica glass and particles formed by aggregation of vaporized silica glass.

✉ Hirofumi Hidai
hidai@faculty.chiba-u.jp

[1] Department of Mechanical Engineering, Chiba University,
Chiba, Japan

1 Introduction

Nanofibers and nanoparticles have recently attracted attention owing to their unique properties, which differ from those of the bulk materials, and are often applied as reinforcements or fillers in composite materials. Another important application of nanomaterials is in catalyst beds, where the large surface area of the nanostructures contributes to high catalytic performance. A diverse range of methods have been reported for the synthesis of nanomaterials. The synthesis of nanoparticles and nanofibers from molten or vaporized materials is particularly important. Some methods rely on laser irradiation to heat a target material or ablate a target. One known issue in such nanoparticle syntheses is that collisions between plasma generated by laser irradiation and ambient air lead to aggregation of the nanoparticles [1]. Laser irradiation can also be used in nanofiber synthesis. Laser irradiation at a sufficiently high laser power induces the target material to melt and the molten material is dispersed into the air owing to the ablation pressure. A variety of fibers have been synthesized by this approach. For example, excimer-laser irradiation of a polymethyl methacrylate targets can generate fibers with diameters of several hundred nanometers [2]. The irradiation of a silica glass target by an ultrafast laser with a high repetition rate has also been reported to generate fibers with diameters less than a few hundred nanometers [3].

The fiber fuse phenomenon has been investigated [4]. Under laser irradiation with a high-power density, edge faces or material defects in a fiber absorb the laser light. The points of absorption are heated and the surrounding glass also starts to absorb laser light, because the rise in temperature increases the absorption of the optical glass. As the glass starts to absorb light the high-temperature

light-absorbing region starts to move toward the light source. A similar phenomenon occurs in bulk glass, where it is termed continuous-wave laser backside irradiation (CW-LBI) [5]. The fiber fuse phenomenon is generally unwelcome; optical fibers are severely damaged through this phenomenon. However, we propose that CW-LBI or the trajectory left by CW-LBI might be useful. We have previously studied the process of CW-LBI, calculated the temperature behavior during the process [6], estimated the mechanical and compositional properties of the modified area formed in glass [7], and developed a technique to drill holes in glass using CW-LBI [8]. In the latter of these studies, we noted that fine fibers were synthesized as byproducts during the drilling process.

In demonstrations of fiber and particle formation reported by other researchers, the products were synthesized from a molten pool or ablation plume generated by laser irradiation of a substrate [9–11]. In our fiber synthesis method using CW-LBI, the primary material was glass produced from a depth of a few millimeters within a substrate. In the drilling process, a hole with a length of several millimeters was drilled into the plasma region at high temperature and pressure. The plasma region, with a length of several millimeters, was confined in the bulk glass and then glass from this confined region was ejected. Hence, the synthesis process occurs through an explosion. Although the use of pulsed lasers is more common, the use of a continuous-wave (CW) laser is a characteristic of this method. We have previously demonstrated another fiber synthesis method using a CW laser [12].

In this paper, we report in situ observations of the fly-off process of materials synthesized by CW-LBI of a glass substrate, scanning electron microscope (SEM) images of the synthesized materials, and micrographs of the substrate after synthesis by CW-LBI. We characterized the synthesized materials, and discuss this fine materials synthesis process based on our findings and previous literature reports.

2 Experimental

The experimental setup used for this research (Fig. 1) was the same as that previously reported [8]. A silica glass substrate with a thickness of 10 mm, copper foil absorbent, and glass slide were contacted and fixed in position with a jig. A CW fiber laser (FLC-300-A, Fujikura, Ltd., Tokyo, Japan) with an oscillation wavelength of 1095 nm was used. The laser power at the front of the substrate surface was set to be 210 W. A mechanical shutter was used to set the irradiation duration to be 0.5 s. The laser was focused on the absorbent by a convex lens with a focal length of 407 mm through the substrate. A high-speed camera
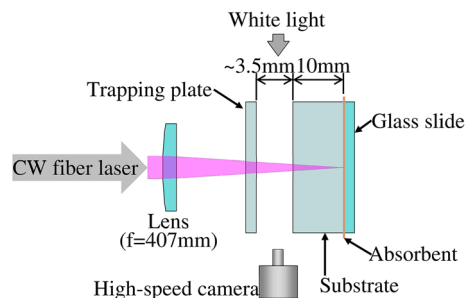

Fig. 1 Schematic of the experimental setup

(Phantom V7.3, Vision Research, Inc., Wayne, NJ, USA) was positioned perpendicular to the laser beam axis to observe shadowgraphs of the process. To trap ejected products, a trapping plate consisting of 3-mm-thick silica glass was placed between the convex lens and substrate. The distance between the trapping plate and the substrate surface was ∼3.5 mm, which enabled ejected materials to be deposited on the trapping plate. The experiments were conducted under ambient conditions.

A previous paper [8] has detailed the ejection process; i.e., the drilling process of silica glass by CW-LBI. The drilling steps are briefly described as follows. Light emission from the absorbent was initiated by laser irradiation. The resulting spot with a high temperature and high pressure featured a spindle shape with a round forefront and sharp rear. The spot propagated in the glass substrate toward the light source without changing the focal position. At the moment when the emission reached the substrate surface on the opposite side of the absorbent, molten glass in the region of the light emission was ejected from the substrate. After the ejection, a spindle-shaped hole remained in the glass substrate.

In this study, the above drilling process was performed, and the ejected materials were trapped and analyzed. The ejected materials were observed with a scanning electron microscope (SEM, S-4700 Hitachi, Tokyo, Japan) after platinum coating. The substrate after the drilling process was also imaged by optical microscopy.

3 Results

3.1 In situ observation

The laser irradiation induced emission from the absorbent in the vicinity of the laser beam. The emission then migrated in the silica glass substrate toward the light source. At the moment when the emission forefront reached the glass surface, material was ejected from the substrate with an audible explosion. This process formed a hole in the silica glass, as has been discussed elsewhere [8].

Figure 2 shows the in situ observation results of the ejection process. A trapping plate was not included in the setup when the in situ observation was conducted. The moment that the light emission forefront reached the substrate surface and ejection was observed on the left side of the substrate was defined as 0 µs. At −157.5 µs, light emission approaching the substrate surface was observed. A long and thin light emission was generated outside of the viewing field, which propagated from the right to the left side of the image. At 0 µs, the plume of ejected material was observed as a dark shadow near to the point where the emission forefront reached the substrate surface. At

15.75 µs, a radially propagating shadow with a radius of ∼5 mm was observed. An expanding plume was observed in the field of view until 47.25 µs. At 31.5 µs, fibrous agglomerated materials were identified in the plume as network-like shadows. The ejection of the fibrous agglomerated materials continued until 126 µs. The emission of light disappeared after 1575 µs.

3.2 Observation of ejected materials

We examined the ejected materials retained by the trapping plate as shown in Fig. 3. The ejected materials were

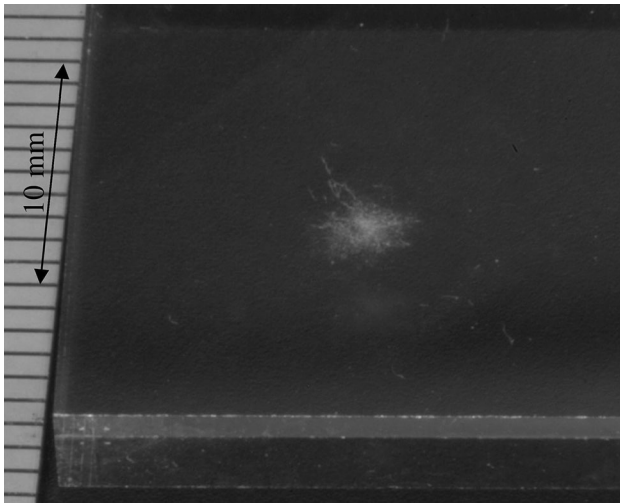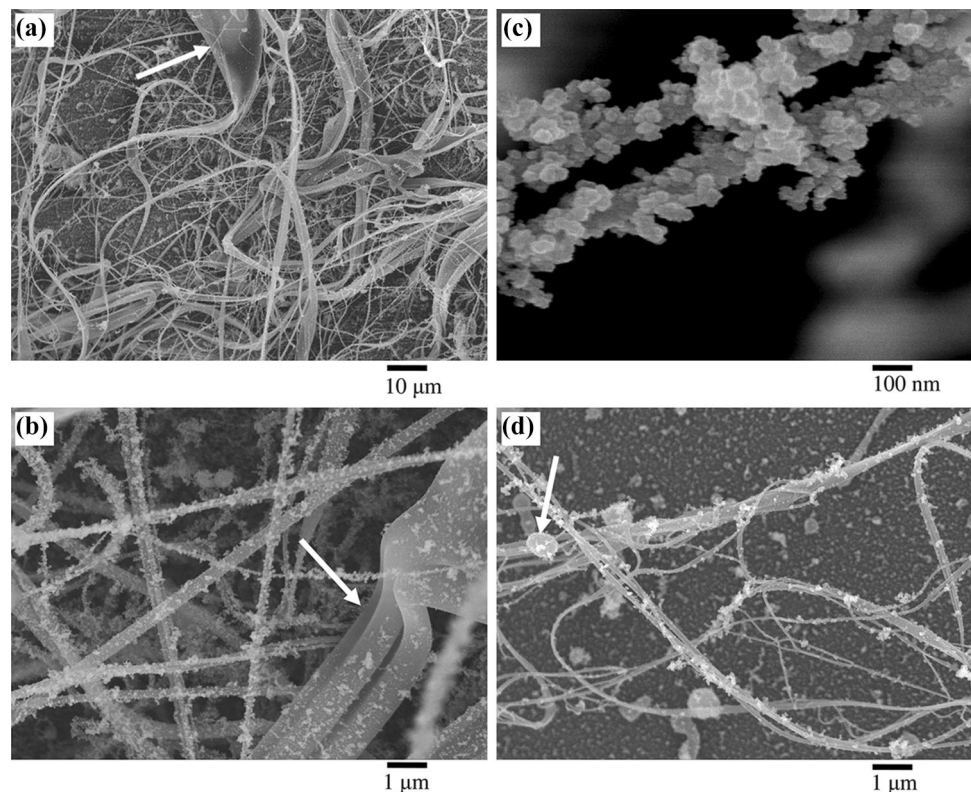**Fig. 2** Images of in situ observations of the drilling process obtained by a high-speed camera
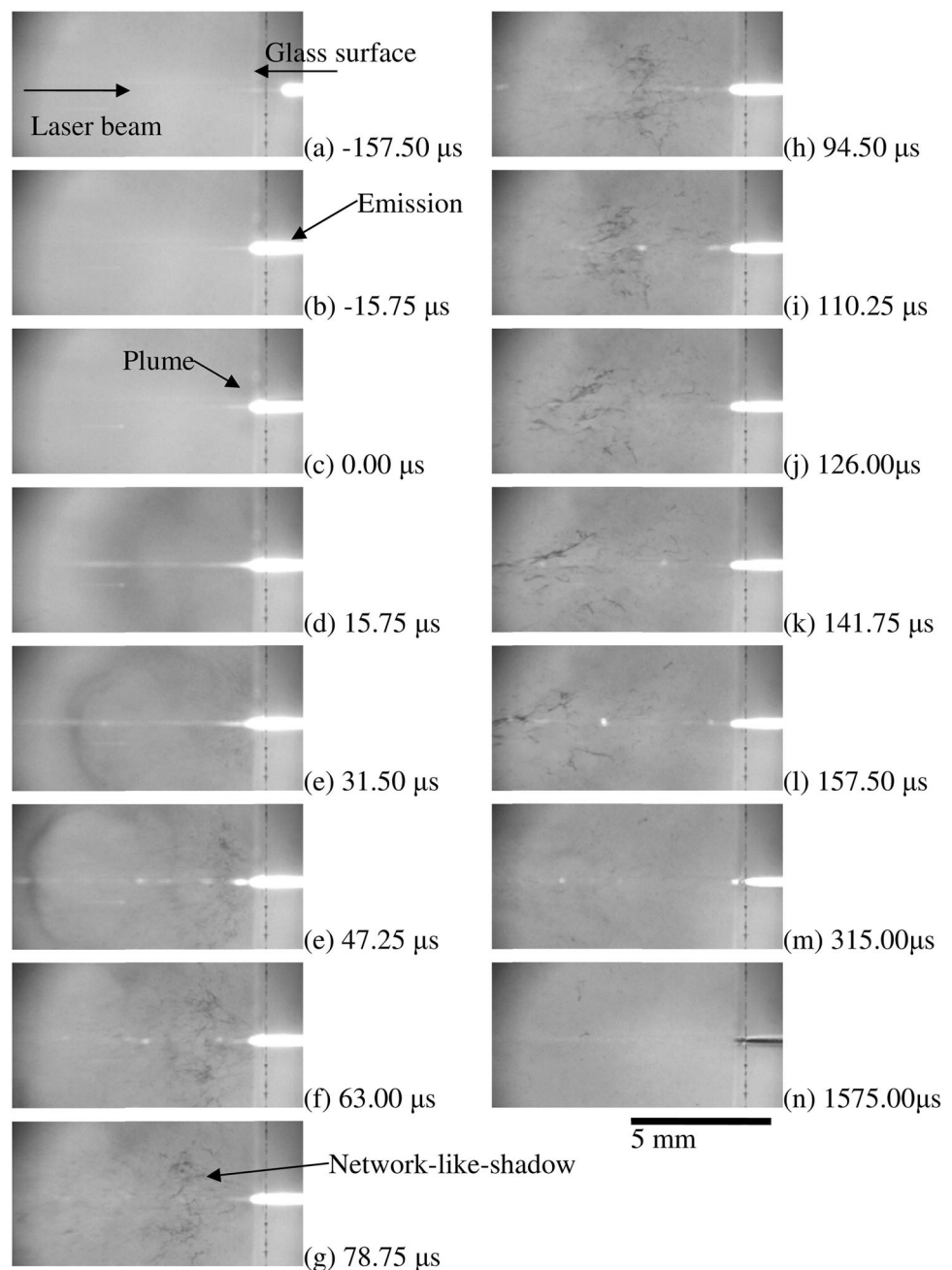
Fig. 3 Photograph of ejected materials from the drilling process retained on trapping plate

visually observable as a white area with a diameter of ~ 4 mm. However, the ejected materials were actually adhered over the whole trapping plate although this is difficult to observe from Fig. 3.

Figure 4 shows SEM images of the ejected materials. Figure 4a–c shows images of an area where the density of the ejected materials was high. Fibers with a wide range of diameters were detected. In Fig. 4a, a fiber with a diameter of more than 10 μm was observed. This thick fiber was

tapered and appeared to be extended. Figure 4b and c shows high-magnification images of the same area. Fibers with diameters of hundreds of nanometers were observed. Figure 4c shows that particles with diameters of tens of nanometers were attached to the fibers. Figure 4d shows an observation from an area featuring a low density of the ejected materials. The densities of both fibers and particles were low. A droplet with a diameter of hundreds of nanometers was observed as indicated by an arrow. Some other droplets were also observed in the field. The droplets were perceived as different from the above-mentioned particles with diameters of tens of nanometers attached to the fibers. Raman and energy-dispersive X-ray spectra of the ejected materials and an unused glass substrate were obtained and compared, as shown in Fig. 5. We found no notable compositional differences in these results.

3.3 Observations of a substrate after the drilling process

Figure 6 shows micrographs of a glass substrate after the drilling process. Figure 6a illustrates the entire trajectory of the drilling process. As described in previous papers, CW-LBI was initiated on the right end face of the substrate, and the generated light emission propagated to the left side, where the light source was positioned [5]. The ejection occurred from the surface of the left side of the substrate

Fig. 4 SEM images of ejected materials. **a** Image of an area with a high density of ejected materials. **b**, **c** High-magnification images of the high-density area in **a**. **d** Image of an area with a low density of ejected materials. Thick fibers, a fiber surface without particles, and droplets are indicated by white arrows in **a**, **b** and **d**, respectively

Fig. 5 Analysis results: **a** Raman spectra of the ejected materials and an unused substrate. **b** Energy-dispersive X-ray spectra of ejected materials and an unused substrate
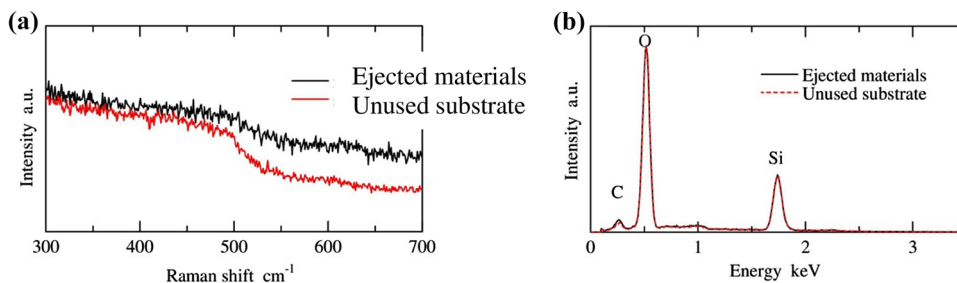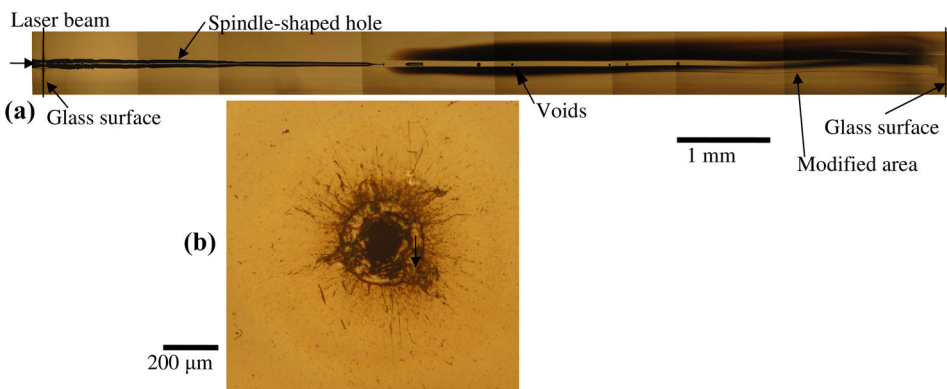

Fig. 6 Micrographs of a substrate after the drilling process. **a** Cross-sectional view of the entire process trajectory. **b** Top-view of the glass surface on the ejection side

when the emission forefront reached the substrate surface [8]. The left side of Fig. 6a shows the spindle-shaped hole, with a depth of ~ 3.8 mm, that was drilled in the substrate. On the right side of the bottom of the hole, a modified area was formed. This modified area was not empty, but solid with a few void regions. Figure 6b shows a micrograph of the ejection hole formed on the substrate surface and indicates that the ejected materials spread radially from the center of the hole.

4 Discussion

In this section, we discuss the synthesis process of the ejected materials through CW-LBI by considering the observed images and comparing them with previous related literature.

Figure 4b and d indicates that the fiber and particle synthesis occurred through different mechanisms. No particles were observed on the as-formed fiber surfaces, as indicated by the arrow in Fig. 4b. The areas without particles remained clear because they were protected from particles by surrounding objects.

The in situ observation results also indicated that two types of phenomena occurred because the ejection process displayed two features, namely plume and network-like shadows. In Fig. 2, a small plume shadow was detected at 0 µs and the plume expanded over time. As discussed later, the plume was the source of particles. From 31.50 µs,
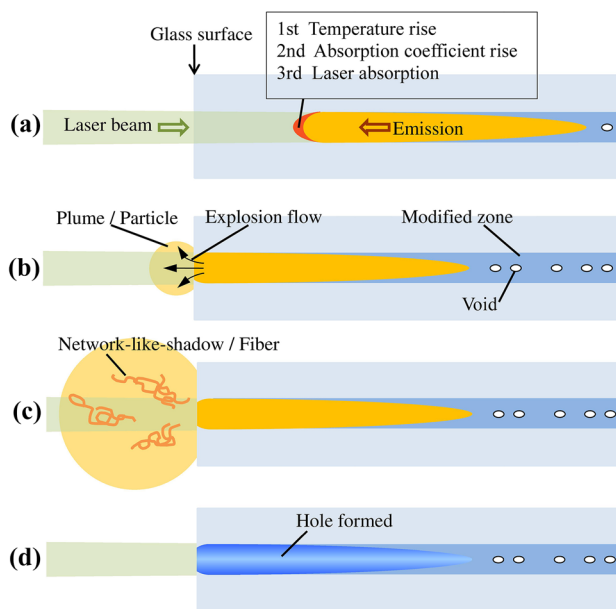

Fig. 7 Illustration of the synthesis process. **a** An emission, generated by the CW-LBI, moves toward the light source. **b** When the emission forefront reaches the glass surface, a plasma plume, which is the material source of particles, is released. **c** Fibers flying off in the expanding plume. **d** Spindle-shaped hole remaining in the substrate

network-like shadows moved outward from the ejection point of the plume as time passed. The network-like shadows were believed to be bunches of fibers, although it is possible that the fibers would not be detected as shadows because the observation resolution was limited. Figure 7

shows an illustration of the synthesis process of the fibers and particles.

The formation of two types of phases was also expected considering the temperature during the drilling process. In the fiber fuse phenomenon, which is similar to CW-LBI, the emission from the fiber core is attributed to the high-density plasma, with an estimated temperature of 5000–10,000 K [4]. Furthermore, for the CW-LBI phenomenon, numerical simulations have been used to estimate the maximum temperature of the emission to be 11,500 K for a glass substrate at a power of 10 W, neglecting thermal radiation and the temperature dependence of the properties [6]. Raman analysis indicated that the fictive temperature of the modified area formed in silica glass by CW-LBI was 1830 K [7]. The above findings suggest that in our experiments using a high-power laser (210 W), the emission area was also a plasma. The formation of a cylindrical molten glass layer between the plasma and the bulk glass during emission propagation is expected. Therefore, two glass phases, i.e., the plasma plume and molten glass, were ejected once the emission forefront reached the substrate surface.

Itoh et al. [10] reported the generation of non-alkaline glass nanofibers using a pulsed-ultraviolet nanosecond laser. During nanofiber generation, a molten pool was observed. They concluded that the nanofibers resulted by growth from the glass substrate. Their SEM observations showed droplets at the edges or middle of fibers. We also detected droplets, as shown in Fig. 4d. Markillie et al. [13] synthesized fibers by a single shot of a CO_2 laser on silica glass. The single-shot radiation formed a crater with fibers attached to the crater wall under certain irradiation conditions. In our experiments, the fibers also extended from the molten glass in the same manner as that reported in Refs. [10] and [13]. The release of the high pressure from the emission region by the explosion is the driving force for fiber extension. The droplets are also deemed to be generated from the molten glass.

Tan and Venkatakrishnan [9] fabricated fibrous nanoparticles by femtosecond laser ablation using several kinds of materials, including glass. During the synthesis process, nanoparticles agglomerated and interwoven fibrous nanostructures formed. Sivakumar et al. [11] demonstrated another synthesis method for glass nanofibers using a femtosecond laser. Attached nanoparticles were observed in some places on the fiber surface. They suggested that the nanofibers grew from molten glass and the nanoparticles were generated by the condensation of vapor in the plasma. In our case, vaporized glass was also the source of the nanoparticles; however, the vaporized glass existed because of the confined plasma, rather than ablation under ambient conditions.

In our developed process, the source material of the fibers and particles came from deep inside the bulk glass substrate, as indicated by the length of the hole that was formed during the process. We have previously demonstrated that the length of the hole increases with laser power to a maximum length of more than 5 mm [8]. Hence, these results are believed to be the first demonstration of fiber or particle synthesis where the material source is deep inside the substrate.

In Fig. 4d, numerous individual particles are observed on the substrate in addition to the fibers. From these features and the above discussion, the drilling process was believed to involve the following steps: Fibers without particles on their surface were synthesized from the molten glass layer in the emission area, becoming enlarged in the explosion flow. The particles were synthesized from vaporized glass. Some of the particles then adhered to the fiber surface, increasing the fiber surface area. Such fibers with a large surface area could be used as a catalyst bed, including a photocatalyst bed or a reformer in fuel cells. The transparency of this material would be particularly beneficial for applications to a photocatalyst bed. Determination of the main forces or physical phenomenon of nanoparticle adhesion and the estimation of the magnitude of the adhesion force will be investigated in the future.

5 Summary

We previously observed the synthesis of silica glass fibers during silica glass drilling using a CW laser [8]. In this paper, we investigated this new fiber synthesis method, which is distinguished from other methods by the material source originating from deep inside the glass bulk and the use of a CW laser as the power source. A high-speed camera allowed in situ observations of the synthesis process. SEM analysis revealed the feature size of the ejected materials. Fibers with particles on their surfaces were observed. The diameter of the fibers ranged from hundreds of nanometers to more than 10 μm. Particles with diameters of tens of nanometers were observed on the fiber surfaces. The ejected materials could be used in catalyst beds because the attached particles increased the surface area of the fibers. Our SEM analysis and in situ observation results indicated that the synthesis process of the ejected materials includes two phases: fiber synthesis and particle synthesis. The fiber synthesis occurs through extraction of molten silica glass with pressure release during explosion. The particle synthesis involved the aggregation of vaporized silica glass.

References

1. M. Ullmann, S. Friedlander, A. Schmidt-Ott, J. Nanoparticle Res. **4**, 499 (2002)
2. V.N. Tokarev, S. Lazare, C. Belin, D. Debarre, Appl. Phys. A **79**, 717 (2004)
3. K. Venkatakrishnan, D. Vipparty, B. Tan, Opt. Express **19**, 15770 (2011)
4. S. Todoroki, *Fiber fuse: light-induced continuous breakdown of silica glass optical fiber* (Springer, Berlin, 2014)
5. H. Hidai, M. Yoshioka, K. Hiromatsu, H. Tokura, Appl. Phys. A **96**, 869 (2009)
6. S. Itoh, H. Hidai, H. Tokura, Appl. Phys. A **112**, 1043 (2013)
7. H. Hidai, M. Yoshioka, K. Hiromatsu, H. Tokura, J. Am. Ceram. Soc. **93**, 1597 (2010)
8. H. Hidai, N. Saito, S. Matsusaka, A. Chiba, N. Morita, Appl. Phys. A **122**, 277 (2016)
9. B. Tan, K. Venkatakrishnan, Opt. Express **17**, 1064 (2009)
10. S. Itoh, M. Sakakura, Y. Shimotsuma, K. Miura, Appl. Phys. B **119**, 519 (2015)
11. M. Sivakumar, K. Venkatakrishnan, B. Tan, Nanoscale Res. Lett. **4**, 1263 (2009)
12. N. Nishioka, H. Hidai, S. Matsusaka, A. Chiba, N. Morita, in *Proceedings of JSPE Spring Meeting* (2017), p. 855
13. G.A.J. Markillie, H.J. Baker, F.J. Villarreal, D.R. Hall, Appl. Opt. **41**, 5660 (2002)